

The article devoted to the 50th anniversary of Konstantin Yu. Zhizhin,
Corresponding Member of the Russian Academy of Sciences

Boron Difluoride β -Diketonates: Structure and Phosphorescence

A. G. Mirochnik^a, E. V. Fedorenko^{a, *}, and A. V. Gerasimenko^a

^a Institute of Chemistry, Far East Branch, Russian Academy of Sciences, Vladivostok, 690022 Russia

*e-mail: gev@ich.dvo.ru

Received December 22, 2022; revised February 9, 2023; accepted February 27, 2023

Abstract—Phosphorescence data on boron difluoride β -diketonates of various structure have been systematized. Nonplanar boron difluoride molecules are characterized by the inversion of the S_1 and T_2 levels, which promotes efficient population of triplet levels and intense phosphorescence or delayed fluorescence of crystals. Planar molecules are characterized by a classical sequence of singlet and triplet levels and a coplanar arrangement of antiparallel molecules, which contributes to excimer delayed fluorescence.

Keywords: boron chelates, structure, luminescence, delayed fluorescence, phosphorescence

DOI: 10.1134/S0036023623600600

Organic dyes exhibiting room-temperature phosphorescence and delayed fluorescence have been actively studied [1–5]. Such materials are candidates for use in design of organic light emitting diodes (OLEDs), chemosensors, temperature sensors, bioimaging, etc. Organic photoluminescent materials are usually considered non-phosphorescent due to extremely weak spin–orbit coupling and high sensitivity to temperature and oxygen access [6]. Boron difluoride β -diketonates, as a rule, exhibit phosphorescence only at low temperatures, when the nonradiative relaxation of the triplet state is inhibited by the low mobility of the dye molecule [7, 8]. For the development of optical functional materials with intense phosphorescence at room temperature, it is important to reveal the relationship between the electronic and geometric structure of phosphors and the efficiency of population of the triplet states of molecules [9, 10].

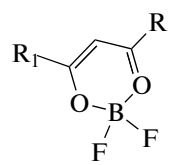
Recently, the room-temperature phosphorescence of boron β -diketonates has been reported [11, 12]. Boron difluoride β -diketonates, unlike most organic compounds, brightly luminesce not only in solution, but also in crystals [13, 14]. Due to their bright luminescence and good photostability in the crystalline state, boron difluoride β -diketonates can be used as a phosphor in OLEDs [15]. Among boron difluoride β -diketonates, there are compounds that have luminescence from bright blue to infrared in the crystalline state. A characteristic feature of boron complexes is the formation of molecularly organized systems in crystals, including dimers, trimers, and aggregates of conjugated molecules, the supramolecular architec-

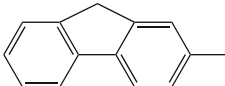
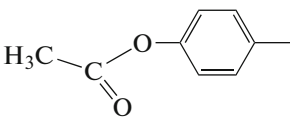
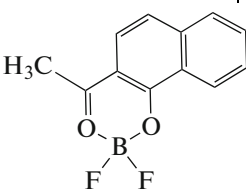
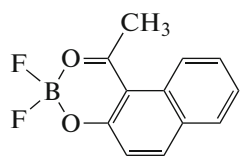
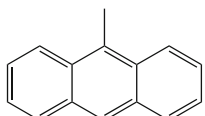
ture of which leads to the emergence of a unique complex of intermolecular interactions, including dimeric (excimeric), interdimeric, and stacking interactions. In this regard, to understand the features of the luminescence of crystalline boron difluoride β -diketonates, it is necessary to compare their spectral and structural characteristics.

This paper presents the results of a comparative analysis of the structure and luminescent properties of some boron difluoride β -diketonates.

EXPERIMENTAL

All compounds were isolated as single crystals, and their unit cell parameters corresponded to the literature data cited in Table 1. The complexes were synthesized and purified in accordance with known procedures [16–22]: by the reaction of the corresponding β -diketonates with boron trifluoride etherate (complexes **2** and **9**) [16]; by acylation of aromatic compounds with acetic anhydride and gaseous boron trifluoride (complexes **1** and **3–5**) [17]; by acylation of α - and β -naphthols with acetic anhydride and boron trifluoride bisacetate (complexes **6** and **7**) [18]; by acylation of *para*-acetoxyacetophenone with acetic anhydride and boron trifluoride α -etherate (complex **8**) [19]; by acylation of α - and β -naphthols with acetic anhydride and boron trifluoride etherate (complexes **10** and **11**) [20]; by the reaction of *ortho*-hydroxydibenzoylmethane with boron trifluoride etherate and butyl borate (complex **12**) [21]; by acylation of anthracene with

Table 1. Luminescent properties of crystals and elements of the crystal structure of complexes **1–13** of general formula


| No. of compound | <i>R</i> | <i>R</i> ₁ | <i>I</i> _{rel.} , arb. units** | λ_{fl} , nm | $\lambda_{DF}^*/\lambda_{phos}$, nm | τ , μ s | Reference, CCDC | Structural element |
|-----------------|---|-------------------------------|---|---------------------|--------------------------------------|------------------|-----------------|---|
| 1 | 2,4,6-(CH ₃) ₃ C ₆ H ₂ | CH ₃ | 116 | 395 | 535 | 0.20 | [28] 794178 | Single molecules, the absence of stacks |
| 2 | C ₆ H ₅ | CH ₃ | 16 | 420/450 | 480/600 | 0.06/0.31 | [30] 1118051 | Stack of antiparallel molecules |
| 3 | <i>p</i> -CH ₃ C ₆ H ₄ | CH ₃ | 120 | 435 | 545 | 0.14 | [31] 184216 | Stack of parallel molecules |
| 4 | <i>p</i> -CH ₃ OC ₆ H ₄ | CH ₃ | 240 | 475 | 495/522 | 0.14 | [32] 184216 | Stack of antiparallel molecules |
| 5 |  | CH ₃ | 7 | 480 | 480/520 | 0.02 | [33] 751758 | Stack of dimers |
| 6 | α -C ₁₀ H ₇ | CH ₃ | | 423 | 463/598 | 33/10* | [18] 721686 | Dimers |
| 7 | β -C ₁₀ H ₇ | CH ₃ | | 537 | 527/607, 667 | 8/17* | [34] 21686 | Stack of dimers |
| 8 |  | CH ₃ | 4 | 400/510 | 550 | 0.23 | This work | Stack of parallel molecules |
| 9 | C ₆ H ₅ | C ₆ H ₅ | 1 | 460/520 | 460/550 | 0.03 | [13] 937594 | Brickwork |
| 10 |  | | – | 520 | – | – | [20] QELWIO1 | Stack of antiparallel molecules |
| 11 |  | | 14 | 450 | 490 | 0.20/1.54 | [20] QELWOU | Dimers |
| 12 | <i>o</i> -HOC ₆ H ₄ | C ₆ H ₅ | 180 | 460 | 535 | 0.10/1.25 | [21] 1866695 | Brickwork |
| 13 |  | CH ₃ | 90 | 555 | 610 | 0.29/1.58 | [22] 653442 | Stacks of anthracene moieties |

* Spectra of asterisked compounds were recorded at 77 K and the spectra of the other compounds, at room temperature.

** The phosphorescence intensity of boron difluoride dibenzoylmethanate **9** was taken to be unity.

acetic anhydride and gaseous boron trifluoride (complex **13**) [22].

1: Colorless crystals, mp 103–104°C. IR (KBr), ν , cm^{-1} : 1611, 1590 (C_6H_4), 1554, 1541 ($\text{C}=\text{O}$, $\text{C}=\text{C}$), 1156, 1138 ($\text{B}-\text{F}$), 1072, 1050 ($\text{B}-\text{O}$). For $\text{C}_{13}\text{H}_{15}\text{BF}_2\text{O}_2$ anal. calcd., %: C, 61.94; H, 6.00. Found, %: C, 61.36; H, 6.09.

2: Colorless crystals, mp 155–156°C. IR (KBr), ν , cm^{-1} : 3138 (OH_{as}), 2928 ($\text{C}-\text{H}_{\text{ph}}$), 1597 ($\text{C}=\text{O}$), 1547 ($\text{C}=\text{C}$), 1439 (CH_3), 1367, 1358 ($\delta_{\text{s}}(\text{B}-\text{O})$), 1156, 1138, 1113 ($\delta(\text{B}-\text{F})$), 1090, 1057 ($\delta_{\text{as}}(\text{B}-\text{O})$). For $\text{C}_{10}\text{H}_9\text{BF}_2\text{O}_2$ anal. calcd., %: C, 55.72; H, 4.78. Found, %: C, 55.96; H, 4.82.

3: Colorless acicular crystals, mp 158–159°C. IR (KBr), ν , cm^{-1} : 1610, 1592 (C_6H_4), 1550, 1510 ($\text{C}=\text{O}$, $\text{C}=\text{C}$), 1164, 1143 ($\text{B}-\text{F}$), 1085, 1050 ($\text{B}-\text{O}$). For $\text{C}_{11}\text{H}_{11}\text{BF}_2\text{O}_2$ anal. calcd., %: C, 58.02; H, 4.95. Found, %: C, 59.32; H, 4.89.

4: Pale yellow translucent crystals, mp 147–149°C. IR (KBr), ν , cm^{-1} : 1606 (C_6H_4), 1561, 1511 ($\text{C}=\text{O}$, $\text{C}=\text{C}$), 1222, 1189 ($\text{B}-\text{F}$), 1085, 1053 ($\text{B}-\text{O}$). For $\text{C}_{11}\text{H}_{11}\text{BF}_2\text{O}_3$ anal. calcd., %: C, 54.82; H, 4.62. Found, %: C, 54.55; H, 4.70.

5: Yellow-orange crystals, mp 260–261°C. IR (KBr), ν , cm^{-1} : 1560, 1543 ($\text{C}=\text{O}$, $\text{C}=\text{C}$), 1152, 1128 ($\text{B}-\text{F}$), 1059, 1024 ($\text{B}-\text{O}$). For $\text{C}_{17}\text{H}_{13}\text{BF}_2\text{O}_2$ anal. calcd., %: C, 68.50; H, 4.40. Found, %: C, 68.63; H, 4.36.

6: Pale yellow translucent crystals, mp 153–155°C. IR (KBr), ν , cm^{-1} : 3145, 3062 ($\text{C}-\text{HAr}$), 1627 (C_{10}H_7), 1598, 1541 ($\text{C}=\text{O}$, $\text{C}=\text{C}$), 1373 ($\text{B}-\text{O}$), 1184, 1155 ($\text{B}-\text{F}$), 1078, 1053 ($\text{B}-\text{O}$). For $\text{C}_{14}\text{H}_{11}\text{BF}_2\text{O}_2$ anal. calcd., %: C, 64.66; H, 4.26. Found, %: C, 64.45; H, 4.22.

7: Bright yellow crystals, mp 182–183°C. IR (KBr), ν , cm^{-1} : 3145, 3064 ($\text{C}-\text{HAr}$), 1627 (C_{10}H_7), 1598, 1542 ($\text{C}=\text{O}$, $\text{C}=\text{C}$), 1373 ($\text{B}-\text{O}$), 1184, 1153 ($\text{B}-\text{F}$), 1078, 1049 ($\text{B}-\text{O}$). For $\text{C}_{14}\text{H}_{11}\text{BF}_2\text{O}_2$ anal. calcd., %: C, 64.66; H, 4.26. Found, %: C, 64.40; H, 4.28.

8: Pale yellow crystals, mp 160–161°C. IR (KBr), ν , cm^{-1} : 1756 ($\text{CH}_3\text{C}=\text{O}$), 1586 (C_6H_4), 1543, 1506 ($\text{C}=\text{O}$, $\text{C}=\text{C}$), 1350 ($\text{B}-\text{O}$), 1197, 1172 ($\text{B}-\text{F}$), 1047, 1012 ($\text{B}-\text{O}$). For $\text{C}_{12}\text{H}_{11}\text{BF}_2\text{O}_4$ anal. calcd., %: C, 53.78; H, 4.14. Found, %: C, 53.74; H, 4.12.

9: Pale yellow translucent crystals, mp 190–191°C. IR (KBr), ν , cm^{-1} : 1595 (C_6H_5), 1547, 1488 ($\text{C}=\text{O}$, $\text{C}=\text{C}$), 1373 ($\text{B}-\text{O}$), 1247, 1153 ($\text{B}-\text{F}$), 1103, 1045 ($\text{B}-\text{O}$). For $\text{C}_{15}\text{H}_{11}\text{BF}_2\text{O}_2$ anal. calcd., %: C, 66.22; H, 4.08. Found, %: C, 66.28; H, 4.11.

10: Orange crystals, mp 193–194°C. IR (KBr), ν , cm^{-1} : 1619, 1599 (C_{10}H_7), 1565, 1530, 1459 ($\text{C}=\text{O}$, $\text{C}=\text{C}$), 1200–1170 ($\text{B}-\text{F}$), 1062–1044 ($\text{B}-\text{O}$). For $\text{C}_{12}\text{H}_9\text{BF}_2\text{O}_2$ anal. calcd., %: C, 61.59; H, 3.88. Found, %: C, 61.61; H, 3.92.

11: Pale yellow translucent crystals, mp 156–157°C. IR (KBr), ν , cm^{-1} : 1627, 1580 (C_{10}H_7), 1545, 1490, 1474 ($\text{C}=\text{O}$, $\text{C}=\text{C}$), 1200–1190, 1062 ($\text{B}-\text{F}$, $\text{B}-\text{O}$). For $\text{C}_{12}\text{H}_9\text{BF}_2\text{O}_2$ anal. calcd., %: C, 61.59; H, 3.88. Found, %: C, 61.56; H, 3.90.

12: Pale yellow crystals, mp 195–196°C. IR (KBr), ν , cm^{-1} : 3459 ($\text{O}-\text{H}$), 1624 (C_6H_5 , C_6H_4), 1566, 1539 ($\text{C}=\text{O}$, $\text{C}=\text{C}$), 1157, 1134 ($\text{B}-\text{F}$), 1083, 1049 ($\text{B}-\text{O}$). For $\text{C}_{15}\text{H}_{11}\text{BF}_2\text{O}_3$ anal. calcd., %: C, 62.54; H, 3.85. Found, %: C, 62.36; H, 3.74.

13: Brown crystals, mp 228–229°C. IR (KBr), ν , cm^{-1} : 1626 (C_{10}H_7), 1571, 1541 ($\text{C}=\text{O}$, $\text{C}=\text{C}$), 1190, 1167 ($\text{B}-\text{F}$), 1086, 1065 ($\text{B}-\text{O}$). For $\text{C}_{18}\text{H}_{13}\text{BF}_2\text{O}_2$ anal. calcd., %: C, 69.23; H, 4.26. Found, %: C, 69.27; H, 4.23.

Melting points were determined on a Buchi Melting Point B-540 instrument. IR spectra were recorded on a Perkin Elmer Spectrum BX 400 FT IR spectrophotometer. Luminescence and luminescence excitation spectra were recorded on a Shimadzu RF 5301 spectrofluorimeter. Phosphorescence spectra and lifetimes at room temperature were recorded on a Agilent Technologies Varian Cary Eclipse spectrometer and at 77 K, on a Fluorolog 3 spectrometer.

X-ray single-crystal diffraction study of crystal **8** recrystallized from acetonitrile was performed on a Bruker SMART-1000 CCD diffractometer with MoK_α radiation at 296(2) K. The collection of experimental data from the sample was carried out in three groups of 906 frames each at angles $\varphi = 0^\circ$, 90° , and 180° by ω -scanning with a step of 0.2° and a counting time of 20 s per frame. The unit cell parameters were refined, and the integrated intensities were recalculated into structural amplitudes using the APEX2 software package [23].

The structure of **8** was determined by direct methods with subsequent refinement of the positional and thermal parameters in the anisotropic approximation for all non-hydrogen atoms using the SHELXTL software [24]. The positions of hydrogen atoms were determined and refined as riding on their parent atoms with a C–H distance of 0.93 Å.

Crystallographic data for $\text{C}_{12}\text{H}_{11}\text{O}_4\text{BF}_2$: a prism ($0.35 \times 0.16 \times 0.10$ mm), monoclinic system, space group Cc , $a = 11.6171(6)$ Å, $b = 11.5684(6)$ Å, $c = 10.4190(5)$ Å, $\beta = 122.097(2)^\circ$, $V = 122.097(2)$ Å³, $Z = 4$, $\rho_{\text{calc}} = 1.501$ g/cm³, $\mu = 0.130$ mm⁻¹, MoK_α radiation ($\lambda = 0.71073$ Å), data were collected in θ range 2.717° – 31.103° , the number of measured reflections (R_{int}) was 13780, the number of reflections with $I \geq 2\sigma(I)$ was 3630, the number of refined parameters was 174; for $I > 2\sigma(I)$, $R_1 = 0.0274$, $wR_2 = 0.0762$; for all reflections, $R_1 = 0.0291$, $wR_2 = 0.0776$.

The crystallographic information was deposited with the Cambridge Crystallographic Data Center under the number CCDC 2225753, from where it can

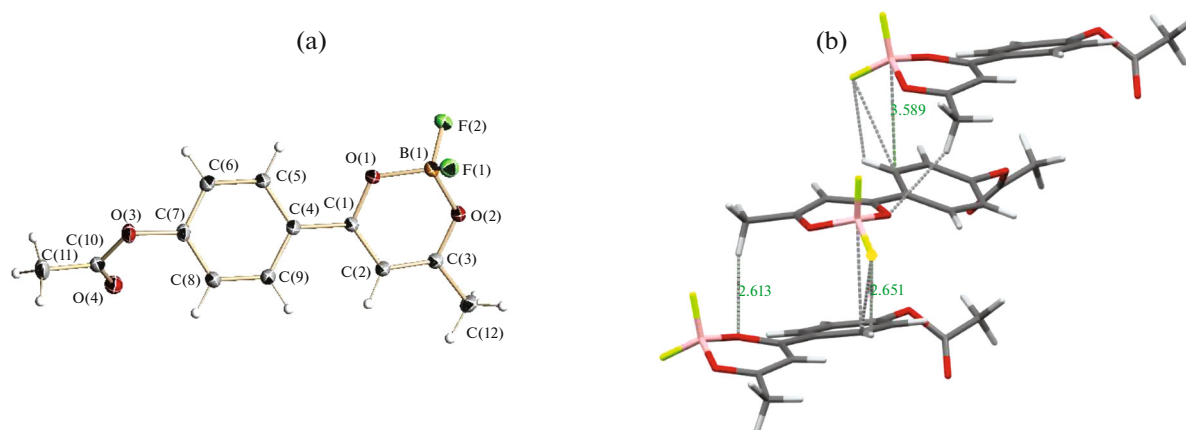


Fig. 1. Crystal structure of complex **8**: (a) molecular structure and (b) stack fragment of the crystal.

be obtained upon request at the website: www.ccdc.cam.ac.uk/data_request/cif.

RESULTS AND DISCUSSION

To study the relationship between the crystal structure and luminescent properties, 13 brightly luminescent crystalline compounds were selected. The crystal structures of twelve of them have been studied earlier (references to the corresponding papers are given in Table. 1).

Figure 1 shows the molecular structure of complex **8** studied in this work. On the one hand, this compound can be considered as an acetate and, on the other hand, as boron difluoride β -diketonate with an

acceptor substituent. The following features should be noted: the molecule is nonplanar, the boron atom and the central carbon atom of the diketonate ring are above the plane of the molecule to give a boat-type conformation. The acetate group is in the *para*-position of the phenyl ring, the angle between the planes of the phenyl ring and the acetate group is 60° ; with this inclination, the n electrons of the O(3) atom weakly interact with the π electrons of the phenyl ring. Molecule **8** contains three atoms that can form hydrogen bonds: fluorine atoms and an oxygen atom of the carboxyl group, which contributes to efficient intermolecular interaction. In the crystal structure of **8**, the molecules are arranged in stacks parallel to the a axis. Inside the stack, a π - π stacking interaction is observed between the phenyl ring of one molecule and the chelate ring of the other (Fig. 1b). Interacting molecules are also connected with neighboring ones by π - π stacking interactions to give a structure of the “skew ladder” type, which is characteristic of J -aggregates. The stacks are interconnected by C-F \cdots H and C=O \cdots H bonds (Fig. 1b), which are typical of crystals of organofluorine compounds [25–27].

For the studied crystals **1–13**, phosphorescence was detected, and for some of them, delayed fluorescence was also observed. Two pairs of isomers (**6** and **7**, **10** and **11**) and compounds **1** and **2**, which have the same structure of the π -system of the molecule, stand out among the studied compounds (Fig. 2). With the same number of π electrons at identical atoms, the compounds differ in geometric structure: in molecules **1**, **6**, and **11**, the aromatic substituent is at an angle to the chelate ring, while molecules **2**, **7**, and **10** of their analogs are flat.

Using the example of compound **2**, which has planar molecules, and compound **1**, the phenyl ring of which is turned by 55° relative to the chelate ring, let us consider the influence of the geometric factor on the deactivation of the excited state in crystals. The presence of methyl substituents in the *ortho* positions

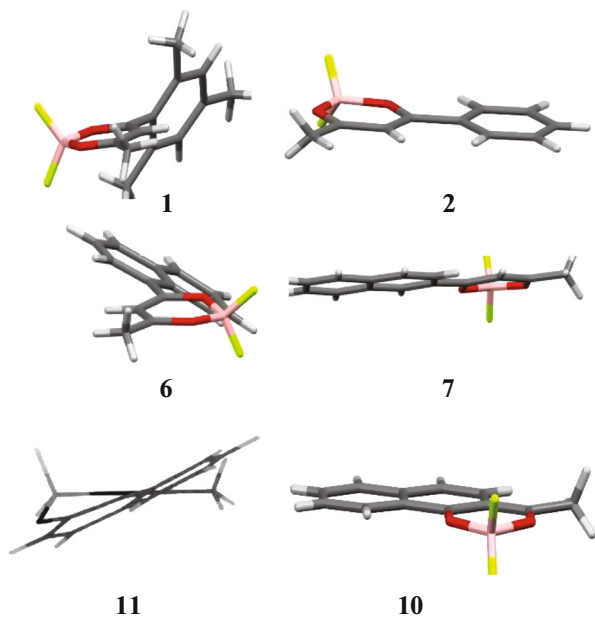


Fig. 2. Structures of complexes **1** and **2**, **6** and **7**, and **10** and **11**.

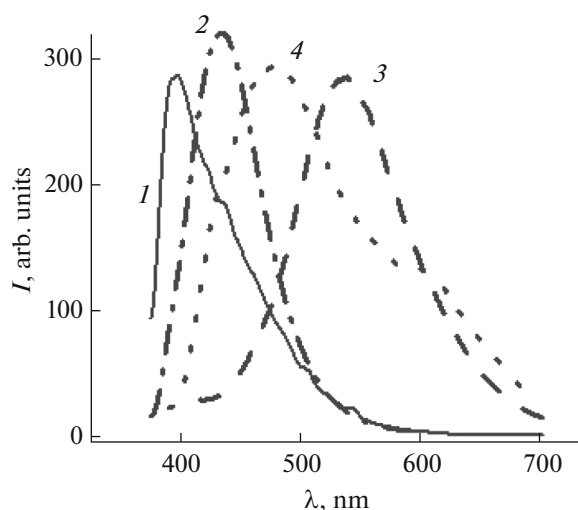


Fig. 3. Luminescence spectra of crystals (1, 3) **1** and (2, 4) **2**: (1, 2) fluorescence and (3, 4) phosphorescence.

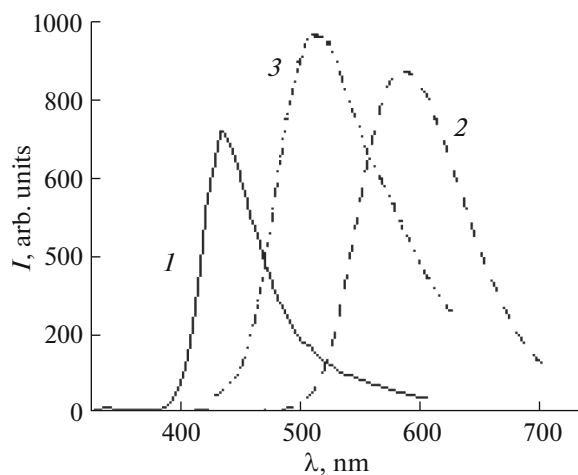


Fig. 4. Luminescence spectra of crystals (1, 2) **11** and (3) **10**: (1, 3) fluorescence and (2) phosphorescence.

of the phenyl ring in **1** leads to a different type of crystal packing compared to **2** and, as a result, to different types of intermolecular interactions [28].

In crystal structure **1**, the phenyl rings of neighboring molecules are arranged to each other in a T-shape, and there is no overlap of the π -systems of neighboring molecules. In crystal structure **2**, molecules are stacked parallel to the c axis, with an intermolecular distance of 3.44 Å, and there is an efficient π - π stacking interaction. Different types of interactions in crystals **1** and **2** lead to the formation of luminescent centers of different nature. Figure 3 shows the fluorescence and phosphorescence spectra of crystals **1** and **2**. For crystals **1**, monomer fluorescence ($\lambda_{\text{max}} = 395$ nm) and phosphorescence ($\lambda_{\text{max}} = 535$ nm, $\tau = 0.20$ μs) are observed (Fig. 3). In the phosphorescence spectrum

of **2**, two bands are observed with maxima at 480 and 600 nm, which are related to delayed excimer fluorescence and phosphorescence, respectively.

The geometry of isomers **10** and **11** is also different. In crystal structure **10**, molecules are planar and stacked with efficient π -stacking interaction resulting in excimer luminescence peaking at 523 nm. Molecules in structure **11** have a bend along the line boron–central carbon atom of the chelate ring and can form only dimers [20]; the maximum of the luminescence spectrum of crystals at 450 nm corresponds to monomer fluorescence. For **10**, phosphorescence and delayed fluorescence are absent. For **11**, phosphorescence is observed with a maximum at 590 nm (Fig. 4).

To reveal the origin of the different ways of deactivation of the electronic excitation energy in the studied isomers, quantum-chemical simulation of molecules **10** and **11** has been performed [29]. For **11**, in contrast to **10**, an inversion of the S_1 and T_2 levels is observed during vibrational relaxation from the geometry S_0 to the optimal geometry S_1 , which is determined by the intersection of the potential energy surfaces in the states S_1 and T_2 . Then, internal conversion $T_2 \rightarrow T_1$ follows, and emission is observed during the $T_1 \rightarrow S_0$ transition (Fig. 5a).

For crystals **6** and **7**, in addition to phosphorescence, delayed fluorescence is observed. For crystals **7**, low-intensity delayed fluorescence and bright phosphorescence are observed, while for crystal **6**, on the contrary, the spectrum is dominated by a delayed fluorescence band coinciding with the fluorescence band of a dilute solution [18] (Fig. 6).

To reveal the origin of the different ways of deactivation of the electronic excitation energy in the studied isomers, quantum-chemical simulation of molecules **6** and **7** has been performed [18]. For **6**, in contrast to **7**, an inversion of the S_1 and T_2 levels is observed during vibrational relaxation from the S_0 geometry to the optimal S_1 geometry, which causes the intersection of the potential energy surfaces in the S_1 and T_2 states (Fig. 5a). For **6**, the inversion of the S_1 and T_2 levels upon relaxation from the S_0 geometry to the optimal S_1 geometry contributes to the population of the T_2 level, phosphorescence through the $T_2 \rightarrow T_1 \rightarrow S_0$ channel, and delayed fluorescence through the $T_2 \rightarrow S_1 \rightarrow S_0$ channel. The delayed fluorescence of crystals **6**, like the fluorescence of **7**, is monomer one [18] (Fig. 6).

For **7**, the classical arrangement of singlet and triplet levels is observed (Fig. 5b). The T_2 level is populated from S_1 ($T_2 \rightarrow T_1 \rightarrow S_0$). The fluorescence of crystals **7** (530 nm) coincides with the excimer fluorescence of solutions with a high concentration of **7** and is of excimer origin. The delayed fluorescence of crystals (531 nm) is also excimer one [18]. The significantly higher intensity and duration of the delayed fluorescence of crystals **6** compared to **7** is worth noting.

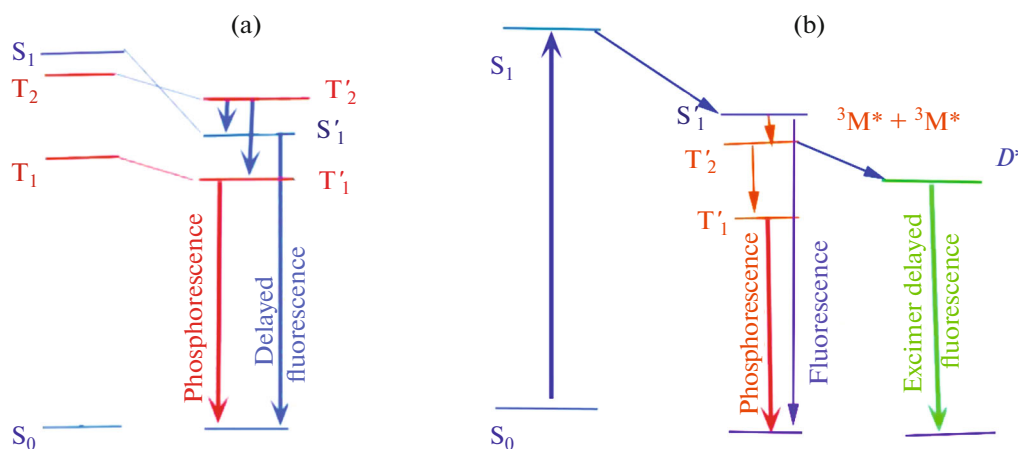


Fig. 5. Diagram of photophysical processes in crystals of (a) nonplanar and (b) planar molecules of boron difluoride β -diketonates.

Thus, the analysis of the luminescent properties of three pairs of compounds—**1** and **2**, **6** and **7**, and **10** and **11**—makes it possible to reveal some regularities. The nonplanar structure of the boron difluoride β -diketonate molecule (**1**, **6**, and **10**) contributes to the inversion of the S_1 and T_2 levels, and intense phosphorescence is observed, which is determined by the intersection of the potential energy surfaces in the S_1 and T_2 states (Fig. 5a). For structures **3**, **8**, **12**, and **13**, in which molecules do not form dimers of antiparallel molecules characteristic of boron difluoride β -diketonates, only phosphorescence is observed (Table 1).

At the same time, the planar structure of molecules, their coplanar arrangement, the classical sequence of singlet and triplet levels, and a small energy gap between S_1 , T_1 , and T_2 contribute to excimer delayed fluorescence. For crystals **2**, **4**, **7**, and **9**,

in which the molecules are planar and have an antiparallel arrangement in stacks favorable for the formation of excimers, intense excimer delayed P-type fluorescence is observed, which occurs because of triplet–triplet annihilation with the formation of an excimer (Fig. 5b)

CONCLUSIONS

Data on the phosphorescent properties of boron difluoride β -diketonates of various structures have been systematized: (1) with planar molecules when the entire molecule lies in the same plane, and (2) with nonplanar molecules when, due to steric hindrance, the aromatic substituent is turned at an angle to the chelate ring. The nonplanar structure of the boron difluoride β -diketonate molecule promotes the inversion of the S_1 and T_2 levels, efficient population of the triplet levels, and intense phosphorescence of the crystals. At the same time, molecules with a planar structure are characterized by a classical sequence of singlet and triplet levels, and a small energy gap between S_1 , T_1 , and T_2 contributes to the population of the triplet level. For planar molecules with antiparallel arrangement in stacks favorable for the formation of excimers, intense excimer delayed P-type fluorescence is observed, which is accompanied by triplet–triplet annihilation to form an excimer. At an arrangement unfavorable for the formation of excimers, phosphorescence of the crystals occurs. The data obtained in this work can be useful for the development of promising luminescent materials with long-lived emission.

FUNDING

The work was supported by the Ministry of Education and Science of the Russian Federation in the framework of State assignment no. FWFN (0205)-2022-0003.

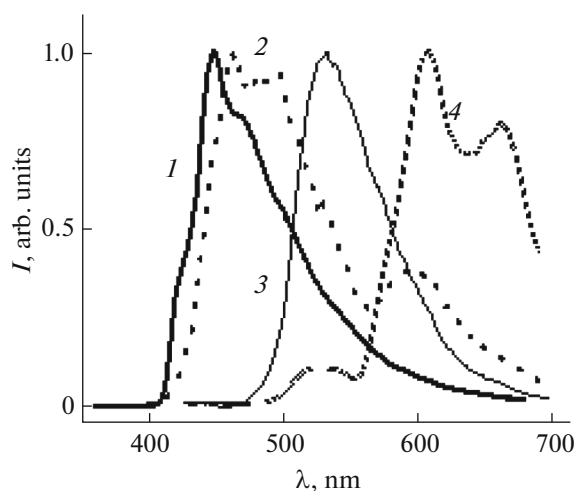


Fig. 6. Luminescence spectra of crystals: (1) fluorescence of **6**, (2) delayed fluorescence of **6**, (3) fluorescence of **7**, and (4) phosphorescence of **7**.

CONFLICT OF INTEREST

The authors declare no conflicts of interest.

REFERENCES

- N. Gan and H. Shi, *Z. An, et al.*, *Adv. Funct. Mater* **28**, 1802657 (2018).
<https://doi.org/10.1002/adfm.201802657>
- T. Zhang, X. Ma, and H. Wu, *Angew. Chem., Int. Ed. Engl.* **28**, 11206 (2020).
<https://doi.org/10.1002/anie.201915433>
- X. Wang, M. Dong, Z. Li, et al., *Dyes Pigm.* **204**, 110400 (2022).
<https://doi.org/10.1016/j.dyepig.2022.110400>
- Z. Wu, J. Nitsch, and T. B. Marder, *Adv. Opt. Mater* **9**, 2100411 (2021).
<https://doi.org/10.1002/adom.202100411>
- T. Y. Chikineva, D. S. Koshelev, A. V. Medved'ko, et al., *Russ. J. Inorg. Chem.* **66**, 170 (2021).
<https://doi.org/10.1134/S0036023621020054>
- H. Ma, A. Lv, L. Fu, et al., *Ann. Phys.* **531**, 1800482 (2019).
<https://doi.org/10.1002/andp.201800482>
- Y. L. Chow, C. I. Johansson, Y. Zhang, et al., *J. Phys. Org. Chem.* **9**, 7 (1996).
- P. Xu, H. Chen, H. Duan, et al., *Russ. J. Gen. Chem.* **92**, 1814 (2022).
<https://doi.org/10.1134/S1070363222090225>
- V. M. Kozenkov, A. A. Spakhov, V. V. Belyaev, et al., *Liq. Cryst.* **16**, 9 (2016).
<https://doi.org/10.18083/LCAppl.2016.4.9>
- V. A. Zhinzhiro and I. E. Uflyand, *Russ. J. Gen. Chem.* **92**, 1937 (2022).
<https://doi.org/10.1134/S1070363222100097>
- G. Zhang, J. Chen, S. J. Payn, et al., *J. Am. Chem. Soc.* **129**, 8942 (2007).
<https://doi.org/10.1021/ja0720255>
- J. Li, X. Wang, X. Zhao, et al., *Chin. J. Chem.* **40**, 2507 (2022).
<https://doi.org/10.1002/cjoc.202200354>
- A. Sakai, M. Tanaka, E. Ohta, et al., *Tetrahedron Lett.* **53**, 4138 (2012).
<https://doi.org/10.1016/j.tetlet.2012.05.122>
- B. Poggi and E. Lopez, et al., *Macromol. Rapid Commun.* **43**, 2200134 (2022).
<https://doi.org/10.1002/marc.202200134>
- B. Domercq, C. Grasso, J.-L. Maldonado, et al., *J. Phys. Chem. B* **108**, 8647.
<https://doi.org/10.1021/jp036779r>
- V. E. Karasev and O. A. Korotkikh, *Zh. Neorg. Khim.* **31**, 869 (1986).
- A. G. Mirochnik, Z. N. Puzyrkov, E. V. Fedorenko, et al., *Russ. J. Inorg. Chem* **67**, 1425 (2022).
<https://doi.org/10.1134/S003602362209008X>
- E. V. Fedorenko, A. G. Mirochnik, A. V. Gerasimenko, et al., *J. Photochem. Photobiol. Chem.* **412**, 113220 (2021).
<https://doi.org/10.1016/j.jphotochem.2021.113220>
- US Pat. 004846; 16.20.2003 Publ.
- B. V. Bukvetskii, E. V. Fedorenko, A. G. Mirochnik, et al., *J. Struct. Chem.* **47**, 56 (2006).
<https://doi.org/10.1007/s10947-006-0265-0>
- E. V. Fedorenko, A. G. Mirochnik, A. V. Gerasimenko, et al., *Dyes Pigm.* **159**, 557 (2018).
<https://doi.org/10.1016/j.dyepig.2018.07.022>
- E. V. Fedorenko, B. V. Bukvetskii, A. G. Mirochnik, et al., *J. Lumin.* **130**, 756 (2010).
<https://doi.org/10.1016/j.jlumin.2009.11.027>
- Bruker. APEX2. Bruker AXS Inc., Madison, 2012.
- Sheldrick G.M. SHELXTL/PC, Versions 5.10, Bruker AXS Inc., Madison, Wisconsin, 1998.
- V. R. Thalladi, H.-C. Weiss, D. Bläser, et al., *J. Am. Chem. Soc.* **12**, 8702 (1998).
<https://doi.org/10.1021/ja981198e>
- A. Brammer, E. Bruton, and P. Sherwood, *Cryst. Growth Des.* **1**, 277 (2001).
<https://doi.org/10.1021/cg015522k>
- D. Rohde, C.-J. Yan, and L.-J. Wan, *Langmuir* **22**, 4750 (2006).
<https://doi.org/10.1021/la053138+>
- E. V. Fedorenko, B. V. Bukvetskii, A. G. Mirochnik, et al., *Russ. Chem. Bull.* **58**, 2240 (2009).
<https://doi.org/10.1007/s11172-009-0312>
- S. A. Tikhonov, E. V. Fedorenko, A. G. Mirochnik, et al., *Spectrochim. Acta A* **214**, 67 (2019).
<https://doi.org/10.1016/j.saa.2019.02.002>
- A. W. Hanson and E. W. Macaulay, *Acta Crystallogr.* **28**, 1961 (1972).
- A. G. Mirochnik, B. V. Bukvetskii, E. V. Gukhman, et al., *J. Fluor.* **13**, 157 (2003).
<https://doi.org/10.1023/A:1022939209971>
- Y. Dromzee, J. Kossanyi, and V. Wintgens, *Z. Kristallogr.* **212**, 372 (1997).
<https://doi.org/10.1524/zkri.1997.212.5.372>
- B. V. Bukvetskii, E. V. Fedorenko, A. G. Mirochnik, et al., *J. Struct. Chem.* **52**, 221 (2011).
<https://doi.org/10.1134/S0022476611010331>
- B. V. Bukvetskii, E. V. Fedorenko, A. G. Mirochnik, et al., *J. Struct. Chem.* **51**, 545 (2010).
<https://doi.org/10.1007/s10947-010-0079-y>

Translated by G. Kirakosyan